Title:

MRI of placenta accreta: diagnostic accuracy and impact of interventional radiology on foetal-maternal delivery outcomes in high-risk women

Short Title:

MRI of placenta accreta: accuracy and impact on delivery outcomes

Authors:

Federica Fiocchi, MD; Azienda ospedaliero - universitaria Policlinico di Modena, Department of Radiology

Filippo Monelli, MD; Azienda ospedaliero - universitaria Policlinico di Modena, Department of Radiology

Giulia Besutti, MD; University of Modena and Reggio Emilia, Clinical and Experimental Medicine PhD program

Federico Casari, MD; Azienda ospedaliero - universitaria Policlinico di Modena, Department of Radiology

Elisabetta Petrella, MD; Azienda ospedaliero - universitaria Policlinico di Modena, Department of Medical and Surgical Sciences for Mothers, Children and Adults

Annarita Pecchi, MD; Azienda ospedaliero - universitaria Policlinico di Modena, Department of Radiology

Cristian Caporali, MD; Azienda ospedaliero - universitaria Policlinico di Modena, Department of Radiology

Emma Bertucci, MD; Azienda ospedaliero - universitaria Policlinico di Modena, Department of Medical and Surgical Sciences for Mothers, Children and Adults

Stefano Busani, MD; Azienda ospedaliero - universitaria Policlinico di Modena, Departement of intensive care medicine

Laura Botticelli, MD; Azienda ospedaliero - universitaria Policlinico di Modena, Departement of Pathology

Fabio Facchinetti, MD; Azienda ospedaliero - universitaria Policlinico di Modena, Department of Medical and Surgical Sciences for Mothers, Children and Adults

Pietro Torricelli, MD; Azienda ospedaliero - universitaria Policlinico di Modena, Department of Radiology

Source of founding:

None of the authors has received any form of founding for the research work or for the publication of the article.

Conflict of interest:

None of the authors has any conflict of interest to declare.

Acknowledgments:

Shaniko Kaleci, PhD (University of Modena and Reggio Emilia, Departement of Dermatology) assisted Filippo Monelli MD in the execution and validation of statistical analysis.

Abstract:

Purpose: To assess accuracy and reproducibility of MRI diagnosis of invasive placentation (IP) in high-risk patients and to evaluate reliability of MRI features. Secondary aim was to evaluate impact of interventional radiology (IR) on delivery outcomes in patients with IP at MRI.

Methods: Twenty-six patients (mean age 36.24y/o,SD6.16) with clinical risk-factors and echographic suspicion of IP underwent 1.5T-MRI. Two readers reviewed images. Gold standard was histology in hysterectomized patients and obstetric evaluation at delivery for patients with preserved uterus. Accuracy and reproducibility of MRI findings were calculated.

Results: Incidence of IP was 50% (13/26) and of PP was 11.54% (3/26). MRI showed 100% sensitivity (95%CI=75.3%-100%) and 92.3% specificity (95%CI=64.0%-100%) in the diagnosis of IP. Gold standard was histology in 10 cases and obstetric evaluation in 16. MRI findings with higher sensitivity were placental heterogeneity, uterine bulging and black intraplacental bands. Uterine scarring, placental heterogeneity, myometrial interruption and tenting of the bladder showed better specificity. MRI inter-rater agreement with Cohen's K was 1. Eleven patients among 14 with MRI diagnosis of IP received IR assistance with positive impact on delivery outcomes in term of blood loss, red cells count, intense care unit length of stay, days of hospitalization and risk of being transfused.

Conclusion: MRI is an accurate and reproducible technique in prenatal diagnosis of IP. MRI helps planning a safe and appropriate delivery eventually assisted by IR, which positively affects foetal and maternal outcomes.

Advances in knowledge: The adoption of MRI evaluation in patients with high risk of invasive placentation allows a more accurate diagnosis in terms of both presence of the disease and its extension to or through or even beyond the myometrium. This led to a better dedicated delivery management with eventual adoption of interventional radiology with a global positive effect on foetal and maternal outcomes.

Title:

MRI of placenta accreta: diagnostic accuracy and impact of interventional radiology on foetal-maternal delivery outcomes in high-risk women

Short Title:

MRI of placenta accreta: accuracy and impact on delivery outcomes

Abstract:

Purpose: To assess accuracy and reproducibility of MRI diagnosis of invasive placentation (IP) in high-risk patients and to evaluate reliability of MRI features. Secondary aim was to evaluate impact of interventional radiology (IR) on delivery outcomes in patients with IP at MRI.

Methods: Twenty-six patients (mean age 36.24y/o,SD6.16) with clinical risk-factors and echographic suspicion of IP underwent 1.5T-MRI. Two readers reviewed images. Gold standard was histology in hysterectomized patients and obstetric evaluation at delivery for patients with preserved uterus. Accuracy and reproducibility of MRI findings were calculated.

Results: Incidence of IP was 50% (13/26) and of PP was 11.54% (3/26). MRI showed 100% sensitivity (95%CI=75.3%-100%) and 92.3% specificity (95%CI=64.0%-100%) in the diagnosis of IP. Gold standard was histology in 10 cases and obstetric evaluation in 16. MRI findings with higher sensitivity were placental heterogeneity, uterine bulging and black intraplacental bands. Uterine scarring, placental heterogeneity, myometrial interruption and tenting of the bladder showed better specificity. MRI inter-rater agreement with Cohen's K was 1. Eleven patients among 14 with MRI diagnosis of IP received IR assistance with positive impact on delivery outcomes in term of blood loss, red cells count, intense care unit length of stay, days of hospitalization and risk of being transfused.

Conclusion: MRI is an accurate and reproducible technique in prenatal diagnosis of IP. MRI helps planning a safe and appropriate delivery eventually assisted by IR, which positively affects foetal and maternal outcomes.

Advances in knowledge: The adoption of MRI evaluation in patients with high risk of invasive placentation allows a more accurate diagnosis in terms of both presence of the disease and its extension to or through or even beyond the myometrium. This led to a better dedicated delivery management with eventual adoption of interventional radiology with a global positive effect on foetal and maternal outcomes.

Abbreviations:

MRI: magnetic resonance imaging

IP: invasive placentation

IR: interventional radiology

GS: gold standard

CS: cesarean section(s)

PA: placenta accreta vera

PI: placenta increta

PP: placenta percreta

BMI: body mass index

SEN: sensitivity

SPEC: specificity

AUROC: area under ROC curve

PPV: positive predictive value

NPV: negative predictive value

IR-A: interventional radiology assisted

IR-NA: interventional radiology non assisted

Hb: haemoglobin

ICU: intense care unit

TSE: turbo spin echo

THRIVE: T1W High Resolution Isotropic Volume Examination

BTFE: balanced turbo field echo

DWI: diffusion weighted images

EPI: echo planar imaging

Introduction

Placental adherence disorders are a relevant cause of maternal morbidity and mortality in peripartum period; among these, invasive placentation (IP) has the most severe clinical impact, which is related to width and depth of myometrial invasion [1, 2]. IP affects about 0.1% of all pregnancies and it comprehends a spectrum of conditions characterized by direct attachment of chorionic villi to the myometrium due to a defect of the spongiosus layer of decidua basalis, which causes increased placental-myometrial adhesion [3, 4]. Three different entities, placenta accreta vera (PA), increta (PI) and percreta (PP) are described figure 1. IP is usually silent throughout pregnancy, but causes 1% of pregnancy related haemorrhages, about 1% of pregnancy related death and 29% of haemorrhages requiring hysterectomy [5, 6, 7].

Incidence of IP is growing in last decades due to an increasing incidence of risk factors [8, 9, 10], namely placenta previa and surgical procedures on the myometrium such as caesarean sections (CS) or other uterine surgery including surgical pregnancy interruptions [11]. Prenatal diagnosis is crucial since in case of IP it is mandatory to plan a CS in a tertiary referral hospital for obstetric surgery with availability of blood products, neonatal - maternal intensive care unit and a skilled multidisciplinary team. In recent years, interventional radiology (IR) assistance through hypogastric or uterine artery occlusion and/or embolization during delivery has been introduced [12, 13, 14, 15] proving to be a safe procedure with few complications and a very low radiation dose administered to the foetus [16, 17].

The main tool for diagnosing IP is targeted ultrasonography performed between the 24th and 26th week [18], whose specificity and sensitivity are both reported over 90% [19]. Nevertheless, diagnostic accuracy of targeted ultrasonography may be affected by operator experience, availability of patient detailed clinical history, posterior implantation of the placenta and obesity [20]. In last two decades, Magnetic Resonance Imaging (MRI) emerged as a diagnostic tool to diagnose IP because, despite its overall equal or even slight lower accuracy [21], it allows a precise description of width and depth of placental invasion. Moreover, MRI does not have the same limitation, and, in case of posterior placentation, obese patients and inconclusive US evaluation its use is suggested by international guidelines [22]. The appropriate time point to perform MRI is as close as possible to the 36th week as, an earlier MRI evaluation underestimates IP [23] and overestimates the presence of placenta previa due to normal ascension of the placenta into the uterus during pregnancy. A later MRI evaluation may overestimate IP and hamper the planning of IR-assisted delivery in women affected by IP.

The first aim of the present study was to assess accuracy and reproducibility of MRI diagnosis of IP in high-risk patients and to evaluate the most accurate feature of IP. In second instance the impact of interventional radiology assistance on delivery outcomes in patients diagnosed with IP at MRI was analysed.

Materials and Methods:

Study design:

A retrospective observational study was conducted on a cohort of consecutive women at intermediate or high risk for IP who underwent to ultrasound evaluation, performed by a dedicated Obstetric Gynaecologist. The study was approved by the ethics committee of the university hospital of Modena and Reggio Emilia.

Patients:

From June 2013 to November 2018, 83 women with suspicion of IP were referred to the Gynaecology Department. The following risk factors were considered: placenta previa, multiple previous caesarean sections or other surgical uterine procedures, posterior placenta, high parity defined as more than 4 pregnancies, maternal age over 35 years and obesity defined as a BMI over 30. The patients received

specific clinical examination and targeted ultrasonography evaluation performed by a dedicated Obstetric Gynaecologist. Twenty-six out of 83 patients were included in the study due to high risk of IP and underwent MRI, which was scheduled before 38th gestational week.

MRI examinations:

All pelvic MRI examinations for placental evaluation were performed on a 1.5T scanner (Philips Achieva, The Best, Netherlands) with 5-element cardiac synergy coil, after injection of an antiperistaltic drug and medium bladder filling. Imaging protocol included single-shot turbo spin-echo T2-weighted (TSE) and steady-state free precession sequences (balanced turbo field-echo BTFE) performed on utero-placental sagittal, axial and coronal planes, T1 weighted high resolution isotropic volume examination fat-saturated (THRIVE) performed on utero-placental axial and sagittal planes. Moreover, a diffusion weighted Echo planar imaging (EPI) was performed in axial plane. Sequences parameters are reported in table 1. In figure 2 a normal placenta is depicted, and features of normal placentation are described.

Images analyses:

Two radiologists, dedicated to pelvic and gynaecological MRI, prospectively evaluated the exams. Readers assigned patients to three groups considering multiple radiological features of IP: non-IP, PA / PI and PP.

Specific features of IP (figure 3) evaluated to formulate MRI diagnosis were: uterine bulging, placental signal heterogeneity, dark intraplacental bands, hyperintense placental lacunae, interruption of the myometrium and of inner myometrial layer, placental implant on previous CS uterine scar and tenting of the bladder [21, 24, 25, 26, 27]. Myometrium Interruption and tenting of the bladder should be considered a sign of extra uterine extension of placental elements typical of PP. PA and PI were considered the same pathology both at US and at MRI, since the difference between them is not possible at imaging.

Interventional Radiology:

All patients with diagnosis of IP at MRI were planned for IR-assisted delivery with the aim to reduce blood loss and related foetal maternal complication. In angiography room, Fogarty occlusion catheters were placed in both hypogastric arteries at their most proximal division with an arterial access gained with Seldinger technique, paying attention to foetal dose exposure. Then, patients were transferred to the operating room, where the CS was performed after the arterial block; in case of difficult afterbirth, uterotonic drugs were administrated. Fetal dose exposure was collected. Delivery-related foetal and maternal outcomes were registered: blood loss, hemoglobin lost in operating room, red cells transfusion, days spent in intense care unit, days of hospitalization, need of transfusion and hysterectomy.

Gold Standard:

A twofold GS [28] was adopted because a precise differentiation between PA and PI is possible only in case of hysterectomy and consequent histopathological evaluation of both placenta and myometrium [29]. Placental histological examination has low reliability for IP assessment [30] and in case of uterus preservation, clinical evaluation of the obstetric surgeon during CS was adopted. In case of hysterectomy, the pathologist was blinded to MRI findings and radiological diagnosis, while in case of surgical GS, the obstetric surgeon was aware of it.

Statistical analysis:

Descriptive statistics were performed for all demographical variables. Numerical data were expressed as mean and standard deviation. Diagnostic performance is evaluated on the ROC curve and the area under the curve (AUC), specificity (SPEC), sensitivity (SEN), PPV and NPV with respective 95% confidence intervals (CI0.95) were calculated for MRI diagnosis of IP, MRI diagnosis of PP and every specific feature of IP.

Cohen's kappa (κ) statistic was calculated in the evaluation of inter-observer agreement. According to the delivery management, women whit MRI diagnosis of IP were subdivided into IR-assisted (IR-A) and IR-not assisted (IR-NA) groups.

Results:

Twenty-six patients with intermediate-high risk of IP at targeted ultrasound underwent MRI: no women were excluded from the study. Five women required an emergency delivery before the planned CS because of foetal complications and three of them diagnosed with IP, could not be assisted with IR. Among 26 patients, 11 underwent hysterectomy and histological examination was performed on removed uterus. In 15 patients, whose uterus was preserved, surgical GS was adopted. At GS, IP was found in 13 patients with an incidence of 50%, and among these, 10 had PA/PI (38.46%) and 3 had PP (11.54%).

Clinical-demographical characteristics grouped for different diagnosis are reported in table 2.

Table 3 summarizes diagnostic accuracy and inter-rater agreement of MRI and MRI specific features evaluated. IP was diagnosed with MRI in 14 patients with 100% sensitivity (CI 0.95: 75.3% - 100%) and 92,3% specificity (CI 0.95: 64.0% - 100%), with one false positive case and no missed diagnosis. The most accurate MRI feature of IP in our case series has been placental heterogeneity followed by uterine bulging and interruption of the myometrium. PP was diagnosed in 3 patients (figure 4) with 66.7% sensitivity (CI 0.95: 9.4% - 99.2%) and 95.6% specificity (CI 0.95: 78.1% - 99.9%) with one false positive case. Moreover, MRI missed a PP, which was evaluated as PI but subsequently showed a focal placental percretism at GS (figure 5).

MRI inter-rater agreement with Cohen's K was 1 (CI 0.95: 1.000 - 1.000).

Among patients with MRI diagnosis of IP, 3 were not assisted with IR and 11 patients were assisted with IR. In table 4 there is a summary of their outcomes. IR-NA group lost 1269.70 ml more blood in the operating room (CI 0.95: 225.87 ml - 2313.53 ml, P=0.0106) and required 794.55 ml red cells transfusion more (CI 0.95: 173.89 ml - 1415.21 ml, P=0.0082). They spent 2 more days in intense care unit (CI 0.95: 0.17 - 3.89, P= 0.0174), stayed 29.67 more days in hospital (CI 0.95: 2.33 - 57.00) and had a relative risk of being transfused of 2.75 (P=0.051). Two outcomes were worse in IR-A group in comparison to IR-NA group: hemoglobin lost in operating room with a difference of 0.22 g (CI 0.95: -1.47 g - 1.91 g, P=0.3894) and the relative risk of being hysterectomized which was 0.81 because 81.18% of IR-A women needed an hysterectomy in comparison to only 66.67% of IR-NA women.

In assisted patients mean time of radiation exposure was 9.84 minutes and mean administrated dose was 121.90 mGy*cm.

Discussion:

MRI allows to describe the exact position of the placenta and its eventual adhesion disorders or extension through the myometrium with high reliability. MRI proved, also in the present study, to be a useful tool in the diagnosis of IP and it should be performed in presence of risk factors, doubtful placental localization and suspected IP as already stated in international guidelines [22]. In the reported case series, MRI was extremely accurate and reproducible in the diagnosis of IP with 100% sensitivity and 92.31% specificity. MRI had an NPV of 100% and a PPV of 92.9%. A high PPV is particularly important in order not to lose any eventual affected patients, while a high PPV allows to avoid over diagnosis and inappropriate IR procedures. Diagnostic accuracy in the recognition of PP is lower, but this result may be affected by the low prevalence in our series. Moreover, MRI diagnosis of IP has a very good reproducibility among dedicated radiologists.

In the present study, the reliability of eight specific MRI features have been evaluated in the diagnosis of IP. The diagnostic performance described in table 3 refers to an MRI exam performed on women with high clinical and sonographic risk of IP.

Two signs can be considered reliable also when present alone: placental heterogeneity and interruption of myometrial layer. Placental heterogeneity regards pathological development of placenta during pregnancy and it is typical of IP. Interruption of myometrial layer indirectly refers to the disruption of muscular fibres, which are substituted by placental elements (Fig. 1) and it is a precise sign of PI or PP depending to the extension of placenta up to or beyond the uterine serosa (Fig. 6). Another sign suggestive of PP is bladder tenting, although its reliability in our case series resulted to be quite low.

The presence of other MRI features of IP should be accurately weighted because they can either represent a sign of IP, a variance from the normality or a sign of other placental disease. In particular uterine bulging and the loss of normal uterine pear shape should be differentiated by placental bulging which can be caused by hypertrophy of a placental lobe and it is quite common at advanced gestational age. Hyperintense placental lacunae in T1 weighted sequences and dark placental bands in T2 weighted images are an expression of the same pathological process and are a sign of placental infraction, typical of IP. They can be seen simultaneously or not depending on the timing of the haemorrhage. Hyperintense placental lacunae should be differentiated by haemorrhagic outcome of a placental abruption, because the former is intraplacental and the latter entities usually lies between placenta and myometrium. Dark intraplacental bands should be differentiated by placental septae, which are thinner and run through the placenta between placental lobes.

Interruption of inner myometrial layer can be considered a reliable sign of IP and in particular of PA because its pathological correlation is a disruption of decidua basalis. It has a quite low specificity because the evaluation of this thin line at advanced gestational age is not easy. Implant on uterine scar can be considered as a specific manifestation of this sign because on previous scar the myometrium is mixed with fibrous tissue and the decidua basalis is frequently interrupted.

The main concern performing MRI and IR on pregnant women was the safety of the mother and the child. Foetal SAR was kept as low as possible to obtain a diagnostic imaging and during IR only fluoroscopy was performed avoiding angiographic imaging. Both procedures are considered safe in the last trimester and are routinely performed in many centres. As regard to fetal SAR, it was not possible to find any clear experimental data on SAR limit or recommended values in pelvic MRI of pregnant women [31, 32]. As regards to IR, we obtained the mean dose administrated which was 121 mGy*cm; considering the absorbed foetal dose 0.15 times the entrance skin dose [33], our values can be considered safe for the mother [34] and the child [35] and in line with the available literature [36].

Our results are consistent with recent studies [37] and metanalysis [38], confirming that MRI evaluation in case of suspected IP at sonography is highly suggested. On the other hand, some authors [39] suggested that US is the only diagnostic tool needed in case of suspected IP when no technical difficulties, like posterior placenta and obesity are present [40]. We partially agree with that but, as shown in many researches through the years, MRI has also a role in defining the grade of IP [41] and eventual extension to other pelvic organs. Moreover, the use of MRI may reduce overdiagnosis and related costs and exposure, for example our case series, 12/26 women with high risk at targeted sonography were then correctly diagnosed as non-IP at MRI examination.

A reliable diagnosis enables to plan and perform a safe delivery in the appropriate setting, which means CS performed before the 40th week of gestational age in a 3rd level hospital with availability of IR assistance, a maternal and neonatal intense care unit and availability of blood products. In our small group of patients diagnosed with IP at MRI, IR assisted delivery reduced bleeding and related morbidity and length of intense

care unit stay and overall hospitalization and the administration of blood products. Two outcomes were worse in the IR-A group: haemoglobin loss in operative room and relative risk of being hysterectomized, although without statistical significance. The count of haemoglobin loss in operating room is probably biased by the fact that patients with higher blood loss, typically IR non-assisted women group, received red cells transfusion, which lowered the global reduction of haemoglobin count. On the other hand, in patients with less blood loss, typically IR assisted women, surgeons and anaesthesiologist tried to avoid risks deriving from transfusion by delaying and frequently avoiding that. The higher relative risk of hysterectomy in the IR assisted group is related to the aim of reducing patient morbidity and not necessarily to preserve uterus, especially in women with high maternal age and/or with a high number of previous caesarean deliveries and surgical uterine procedures.

A limitation of our study is the low number of patients included and especially the low number of women affected whom IR assistance was possible. Women who did not received an IR assistance due emergency delivery had an overall worse condition related also to the emergency delivery and that could have biased our results. No maternal or foetal complication were reported.

Source of founding:

None of the authors has received any form of founding for the research work or for the publication of the article.

Conflict of interest:

None of the authors has any conflict of interest to declare.

References:

1. Jauniaux E, Collins S and Burton GJ (2018) Placenta accreta spectrum: pathophysiology and evidence-based anatomy for prenatal ultrasound imaging, Am J Obstet Gynecol 218(1):75-87.

2. Jauniaux E, Jurkovic D (2012) Placenta accreta: pathogenesis of a 20th century iatrogenic uterine disease. Placenta 33(4):244-51.

3. Kaplan CG (2007) Color Atlas of Gross Placental Pathology 2nd edn. Springer.

4. Faye-Petersen OM, Heller DS, Joshi VV (2006) Handbook of Placental Pathology 2nd edn. Taylor & Francis.

5. Creanga AA, Syverson C, Seed K, Callaghan WM (2017) Pregnancy-Related Mortality in the United States, 2011-2013. Obstet Gynecol, 130(2):366-373

6. Mehrabadi A, Hutcheon JA, Liu S, et al. (2015) Contribution of placenta accreta to the incidence of postpartum hemorrhage and severe postpartum hemorrhage'. Obstet Gynecol 125(4):814-21.

7. Stivanello E, Knight M, Dallolio L, Frammartino B, Rizzo N, Fantini MP (2010) Peripartum hysterectomy and cesarean delivery: A population-based study. Acta Obstet Gynecol Scand 89(3):321-7.

8. Wu S, Kocherginsky M and Hibbard JU (2005) Abnormal placentation: Twenty-year analysis. Am J Obstet Gynecol 192(5):1458-61.

9. Morlando M, Sarno L, Napolitano R et al. (2013) Placenta accreta: incidence and risk factors in an area with a particularly high rate of cesarean section. Acta Obstet Gynecol Scand, 92(4):457-60.

10. Thurn L, Lindqvist PG, Jakobsson M et al. (2016) Abnormally invasive placenta—prevalence, risk factors and antenatal suspicion: results from a large population-based pregnancy cohort study in the Nordic countries. BJOG 123(8), 123(8):1348-55.

11. Silver RM, Landon MB, Rouse DJ et al. (2006) Maternal morbidity associated with multiple repeat cesarean deliveries. Obstet Gynecol 107(6):1226-32.

12. Li K, Zou Y, Sun J, Wen H (2018) Prophylactic balloon occlusion of internal iliac arteries, common iliac arteries and infrarenal abdominal aorta in pregnancies complicated by placenta accreta: a retrospective cohort study. Eur Radiol 28(12):4959-4967.

13. Angileri SA, Mailli L, Raspanti C, Ierardi AM, Carrafiello G, Belli AM (2017) Prophylactic occlusion balloon placement in internal iliac arteries for the prevention of postpartum haemorrhage due to morbidly adherent placenta: short term outcomes. Radiol Med 122(10):798-806.

14. Giurazza F, Albano G, Valentino L et al. (2018) Predelivery uterine arteries embolization in patients affected by placental implant anomalies. Radiol Med 123(1):71-78.

15. Clausen C, Stensballe J, Albrechtsen CK, Hansen MA, Lönn L, Langhoff-Roos J (2013) Balloon occlusion of the internal iliac arteries in the multidisciplinary management of placenta percreta. Acta Obstet Gynecol Scand 92(4):386-91

16. Soro MP, Denys A, de Rham M, Baud D (2017) Short & long term adverse outcomes after arterial embolisation for the treatment of postpartum haemorrhage: a systematic review. Eur Radiol. 27(2):749-762.

17. Manninen AL, Ojala K, Nieminen MT, Perälä J. (2014) Fetal radiation dose in prophylactic uterine arterial embolization. Cardiovasc Intervent Radiol 37(4):942-8.

18. D'Antonio F, Palacios-Jaraquemada J, Lim PS et al. (2016) Counseling in fetal medicine: Evidence-based answers to clinical questions on morbidly adherent placenta. Ultrasound Obstet Gynecol 47(3):290-301.

19. D'Antonio F, Iacovella C, Bhide A (2013) Prenatal identification of invasive placentation using ultrasound: Systematic review and meta-analysis. Ultrasound Obstet Gynecol 42(5):509-17.

20. Bowman ZS, Eller AG, Kennedy AM et al. (2014) Accuracy of ultrasound for the prediction of placenta accreta. Am J Obstet Gynecol 211(2):177.e1-7.

21. D'Antonio F, Iacovella C, Palacios-Jaraquemada J, Bruno CH, Manzoli L, Bhide A (2014) Prenatal identification of invasive placentation using magnetic resonance imaging: systematic review and meta-analysis. Ultrasound Obstet Gynecol 44(1):8-16.

22. Cantwell R, Clutton-Brock T, Cooper G et al. (2011) Saving Mothers' Lives: Reviewing maternal deaths to make motherhood safer: 2006-2008. The Eighth Report of the Confidential Enquiries into Maternal Deaths in the United Kingdom. BJOG 118 Suppl 1:1-203.

23. Horowitz JM, Berggruen S, McCarthy RJ et al. (2015) When timing is everything: Are placental mri examinations performed before 24 weeks' gestational age reliable?. AJR Am J Roentgenol 205(3):685-92.

24. Baughman WC, Corteville JE, Shah RR (2008) Placenta Accreta: Spectrum of US and MR Imaging Findings. RadioGraphics 28(7):1905-16.

25. Lax A, Prince MR, Mennitt KW, Schwebach JR, Budorick NE (2006) The value of specific MRI features in the evaluation of suspected placental invasion. Magn Reson Imaging 25(1):87-93.

26. Alamo L, Anaye A, Rey J et al. (2013) 'Detection of suspected placental invasion by MRI: Do the results depend on observer' experience? Eur J Radiol 82(2):e51-7.

27. Bour L, Placé V, Bendavid S et al. (2014) Suspected invasive placenta: evaluation with magnetic resonance imaging. Eur Radiol 24(12):3150-60.

28. Yang A, Xiao XH, Wang ZL, Wang ZY, Wang KY (2018) T2-weighted balanced steady-state free procession MRI evaluated for diagnosing placental adhesion disorder in late pregnancy. Eur Radiol 28(9):3770-3778.

29. Dannheim K, Shainker SA, Hecht JL (2016) Hysterectomy for placenta accreta; methods for gross and microscopic pathology examination. Arch Gynecol Obstet 293(5):951-8.

30. Benirschke K, Burton GJ, Baergen RN, (2012) Pathology of the Human Placenta, 6th edn. Springer.

31. American College of Radiology, ACR (2015) ACR–SPR practice parameter for the safe and optimal performance of fetal magnetic resonance imaging (MRI). American College of Radiology, 1076(3):1–14.

32. Ray JG, Vermeulen MJ, Bharatha A, Montanera WJ, Park AL (2016) Association between MRI exposure during pregnancy and fetal and childhood outcomes. JAMA 6;316(9):952-61.

33. El-Khoury GY, Madsen MT, Blake ME, Yankowitz J (2003) A New Pregnancy Policy for a New Era. AJR 181:335-340.

34. Nikolic B, Spies JB, Lundsten MJ, Abbara S (2000) Patient radioation dose associated with uterine artery embolization. Radiology 214:121-125.

35. ICRP Publication 103 (2007) The 2007 Recommendations of the International Commission on Radiological Protection. Annals of ICRP.

36. Chen L, Wang X, Li Q, et al (2019) Clinical evaluation of prophylactic abdominal aortic balloon occlusion in patients with placenta accreta: a systematic review and meta-analysis. BMC Pregnancy and Childbirth. 15;19(1):30

37. Maurea S, Romeo V, Mainenti PP et al. (2018) Diagnostic accuracy of magnetic resonance imaging in assessing placental adhesion disorder in patients with placenta previa: Correlation with histological findings. Eur J Radiol 106:77-84.

38. Familiari L, Liberati M, Lim P, et al (2018) 'Diagnostic accuracy of magnetic resonance imaging in detecting the severity of abnormal invasive placenta: a systematic review and meta-analysis. Acta Obstet Gynecol Scand. 97(5):507-520

39. Berkley, EM and Abuhamad, AZ (2013) Prenatal diagnosis of placenta accreta: Is sonography all we need? J Ultrasound Med 32(8):1345-50.

40. McLean LA, Heilbrun ME, Eller AG, Kennedy AM, Woodward PJ (2011) Assessing the Role of Magnetic Resonance Imaging in the Management of Gravid Patients at Risk for Placenta Accreta. Acad Radiol 18(9):1175-80.

41. Aitken K, Allen L, Pantazi S, Kingdom J, Keating S, Pollard L et al. (2016) MRI Significantly Improves Disease Staging to Direct Surgical Planning for Abnormal Invasive Placentation: A Single Centre Experience. J Obstet Gynaecol Can 38(3):246-251.e1.

TABLES

Table 1: MRI protocol.

Exam protocol adopted for MRI evaluation of every patients. It was adapted to every woman, but in some cases, not every sequence could be performed.

Table 2: Study population.

Clinical characteristics of enrolled patients grouped for GS diagnosis. °Uterine surgery is the sum of every surgical event on the uterus including caesarean sections and surgical pregnancy interruptions; * BMI is referred to the beginning of the pregnancy.

Table 3: Accuracy and interrater agreement of MRI.

SEN: sensitivity, SPEC: specificity, AUROC: area under ROC curve, PPV: positive predictive value, NPV: negative predictive value. Cohen's K coefficient: < 0 less than chance agreement; 0.01–0.20 slight agreement; 0.21– 0.40 fair agreement; 0.41–0.60 moderate agreement; 0.61–0.80 substantial agreement; 0.81–0.99 almost perfect agreement; 1 perfect agreement.

Table 4: Efficacy of interventional radiology assistance of the delivery.

Comparison between patients assisted (IR-A) and non-assisted (IR-NA). Hb: Haemoglobin, ICU: Intense care unit, rr: relative risk.

Figure 1: Three histological samples of human placenta. A) Haematoxylin and eosin stain of placenta accreta vera: chorionic villi (black square) are attached to myometrium composed of spindle cells (black circle), throughout decidua basalis (black arrows) which is thinned, but not interrupted. B) Desmin stain of a placenta increta: chorionic villi (black square) infiltrate the myometrium (black circle); decidua basalis cannot be identified. C) Haematoxylin and eosin stain of placenta percreta: chorionic villi (black square and black arrows) penetrate through the myometrium (black circle) up to the uterine serosa.

Figure 2: Patient n° 7, 39 y/o at 32nd week, at 1st pregnancy. Placenta previa with no IP. A) Sagittal BTFE image of a previa posterior placenta. Internal cervical os (white arrow) and cervical canal (white circle). No uterine bulge and normal placental septae (empty arrow), which are thin hypointense lines located between placental lobes. B) Axial T2 wheighted TSE image. Placenta has an homogeneus intermediate T2 signal (white arrows) and lays on the myometrium (white arrowhead), normally thinned at advamced maternal age.

Figure 3. Patient n° 2, 40 y/o at 33rd week, at 11th pregnancy, with 1 previous CS. Placenta previa increta histologically confirmed. A) sagittal BTFE, B) axial T2 TSE, C) BTFE coronal images. A) uterine posterior bulging (white arrow) and implant of the placenta on uterine scar from previous caesarean section, where the myometrium is thinned (black arrowhead). No clear separation between placenta and the cervix (white circle). B) nodular T2 black band (black arrow) in a mild heterogeneous portion of the placenta; C) nodular and thick linear areas of hypointensity (blackarrow) inside a very heterogeneous portion of the placenta and thinning of the inner myometrial layer (black arrowhead).

Figure 4: patient n° 18, 32 y/o at 35th week, at 3rd pregnancy, with 2 previous CS. Placenta previa percreta histologically confirmed. A) BTFE axial and B) T1 GE coronal images. A) penetration of the placental tissue through the myometrium which results interrupted (white arrowhead) and intraplacental nodular black band (white empty arrow) which correspond in B) to an hyperintense T1 spot (white arrow) representing a focus of haemorrhage typical of abnormal placentation.

Figure 5: patient n° 5, 26 y/o at 29th week, at 1st pregnancy, with no previous CS. Placenta previa percreta histologically confirmed. T2 weighted coronal image. Nodular black band (arrowhead) inside a highly heterogeneous portion of the placenta (white dotted circle). On the left side of the uterus, the myometrium is interrupted (white arrows) and it is clear if compared with the opposite side where the myometrium is normal (empty arrow).

Figure 6: patient 10, 26 y/o at 39th week, at 3rd pregnancy, with 2 previous CS. Marginal placenta previa percreta histologically confirmed. BTFE images A) coronal, B) sagittal. Big placental bulge (arrows), nodular T2 dark band (arrowheads), tenting of the bladder (empty arrows).

Section & Topic	No	Item	Reported on page #
TITLE OR ABSTRACT			
	1	Identification as a study of diagnostic accuracy using at least one measure of accuracy (such as sensitivity, specificity, predictive values, or AUC)	1
ABSTRACT			
	2	Structured summary of study design, methods, results, and conclusions (for specific guidance, see STARD for Abstracts)	2
INTRODUCTION			
	3	Scientific and clinical background, including the intended use and clinical role of the index test	4
	4	Study objectives and hypotheses	4
METHODS			
Study design	**5**	Whether data collection was planned before the index test and reference standard were performed (prospective study) or after (retrospective study)	4
Participants	**6**	Eligibility criteria	4-5
	7	On what basis potentially eligible participants were identified (such as symptoms, results from previous tests, inclusion in registry)	4-5
	8	Where and when potentially eligible participants were identified (setting, location and dates)	4-5
	9	Whether participants formed a consecutive, random or convenience series	4
Test methods	**10a**	Index test, in sufficient detail to allow replication	5
	10b	Reference standard, in sufficient detail to allow replication	5
	11	Rationale for choosing the reference standard (if alternatives exist)	5
	12a	Definition of and rationale for test positivity cut-offs or result categories of the index test, distinguishing pre-specified from exploratory	5
	12b	Definition of and rationale for test positivity cut-offs or result categories of the reference standard, distinguishing pre-specified from exploratory	5
	13a	Whether clinical information and reference standard results were available to the performers/readers of the index test	5
	13b	Whether clinical information and index test results were available to the assessors of the reference standard	5
Analysis	**14**	Methods for estimating or comparing measures of diagnostic accuracy	5
	15	How indeterminate index test or reference standard results were handled	5
	16	How missing data on the index test and reference standard were handled	5
	17	Any analyses of variability in diagnostic accuracy, distinguishing pre-specified from exploratory	5
	18	Intended sample size and how it was determined	5
RESULTS			
Participants	**19**	Flow of participants, using a diagram	6
	20	Baseline demographic and clinical characteristics of participants	6
	21a	Distribution of severity of disease in those with the target condition	6
	21b	Distribution of alternative diagnoses in those without the target condition	6
	22	Time interval and any clinical interventions between index test and reference standard	6
Test results	**23**	Cross tabulation of the index test results (or their distribution) by the results of the reference standard	6
	24	Estimates of diagnostic accuracy and their precision (such as 95% confidence intervals)	6
	25	Any adverse events from performing the index test or the reference standard	6
DISCUSSION			
	26	Study limitations, including sources of potential bias, statistical uncertainty, and generalisability	7
	27	Implications for practice, including the intended use and clinical role of the index test	6-7
OTHER INFORMATION			
	28	Registration number and name of registry	x
	29	Where the full study protocol can be accessed	7
	30	Sources of funding and other support; role of funders	7

Fig. 5

Click here to access/download;Figure;5.jpg

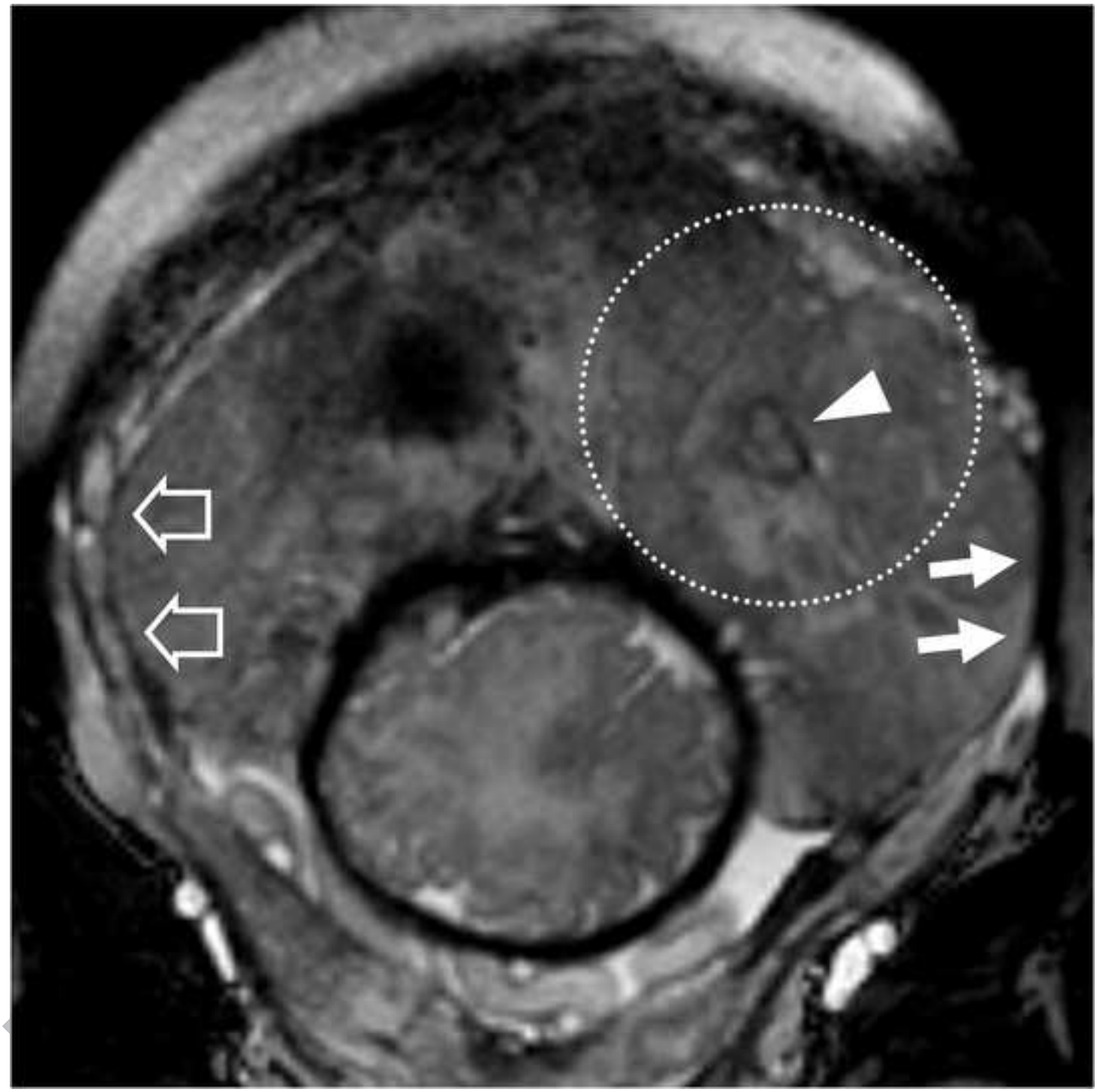

Fig. 6

Click here to access/download;Figure;6AB.jpg

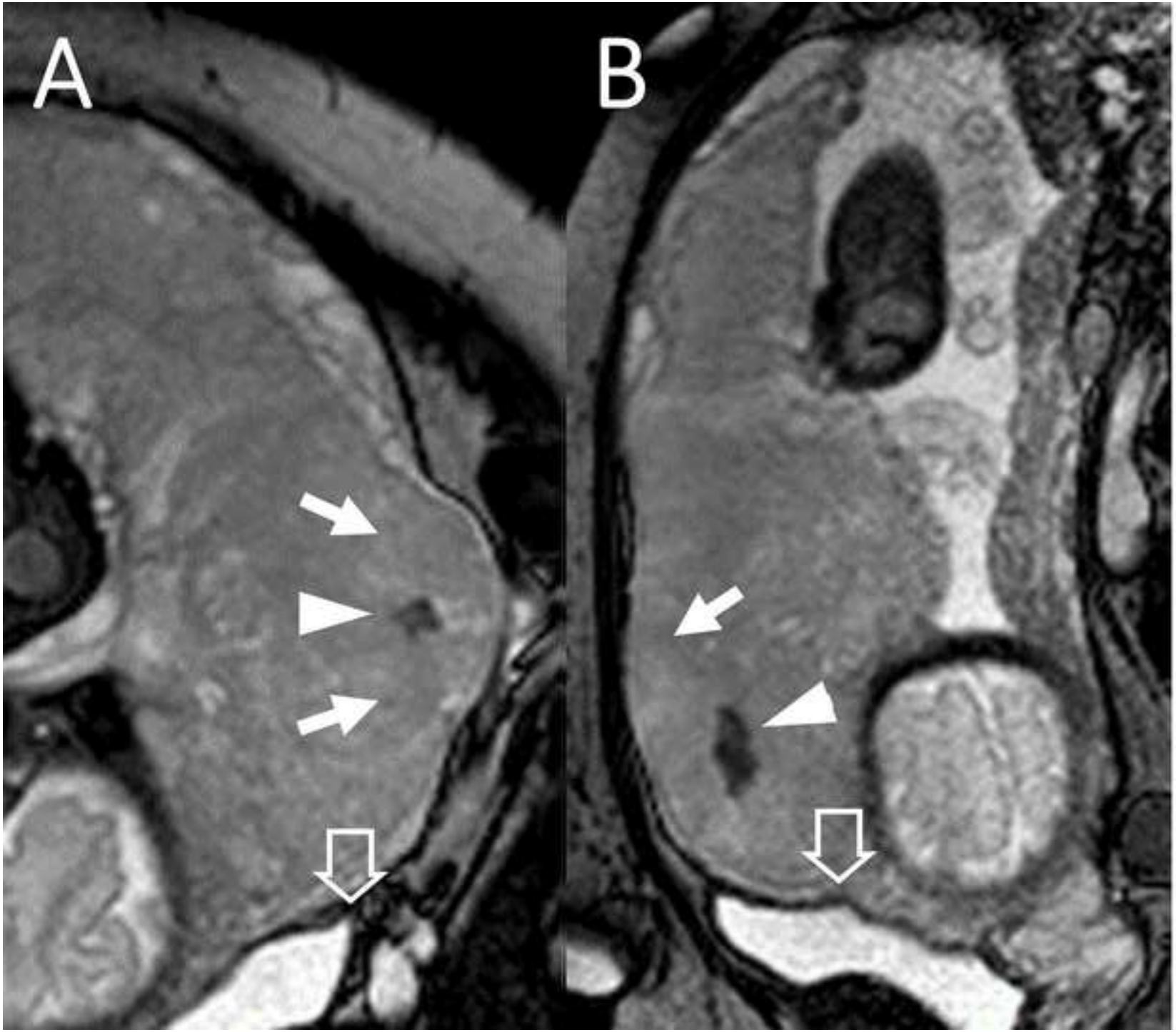

Fig. 1

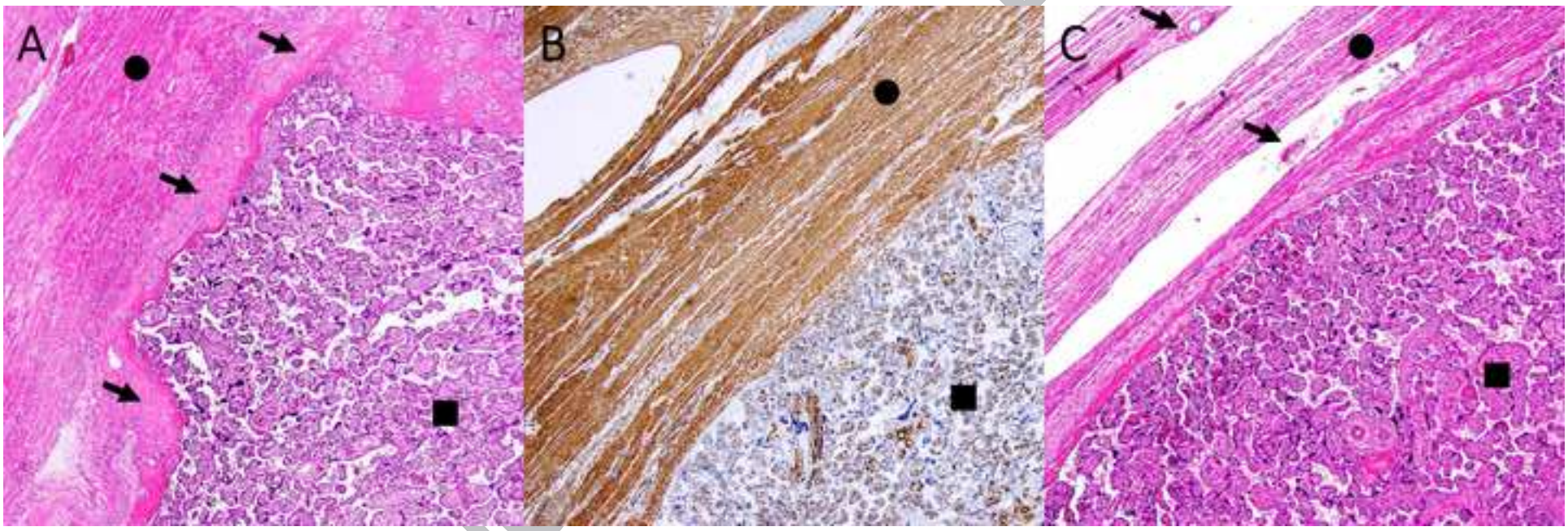

Fig. 2

Click here to access/download;Figure;2AB.jpg

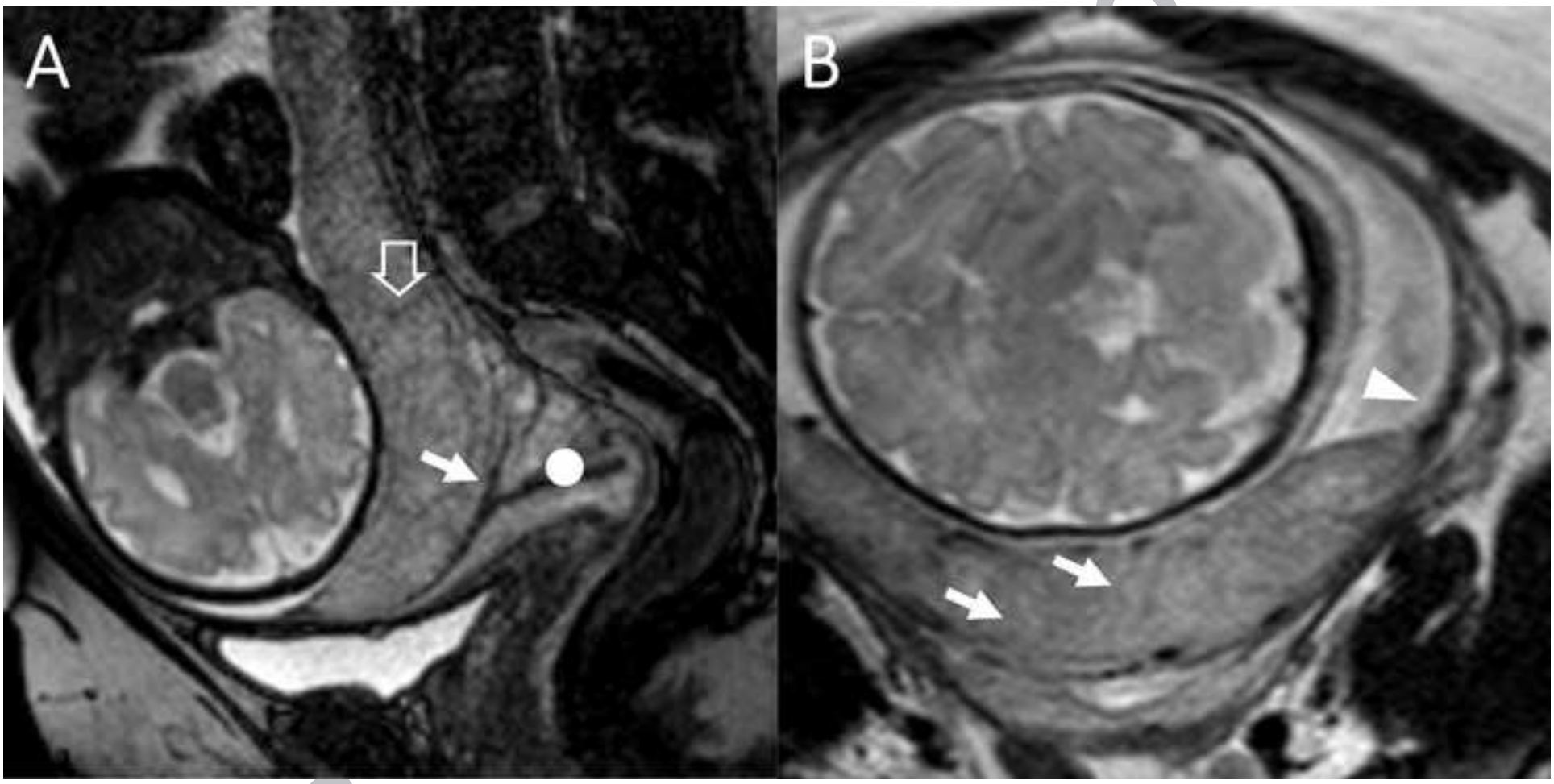

Fig. 3

Click here to access/download;Figure;3ABC.jpg

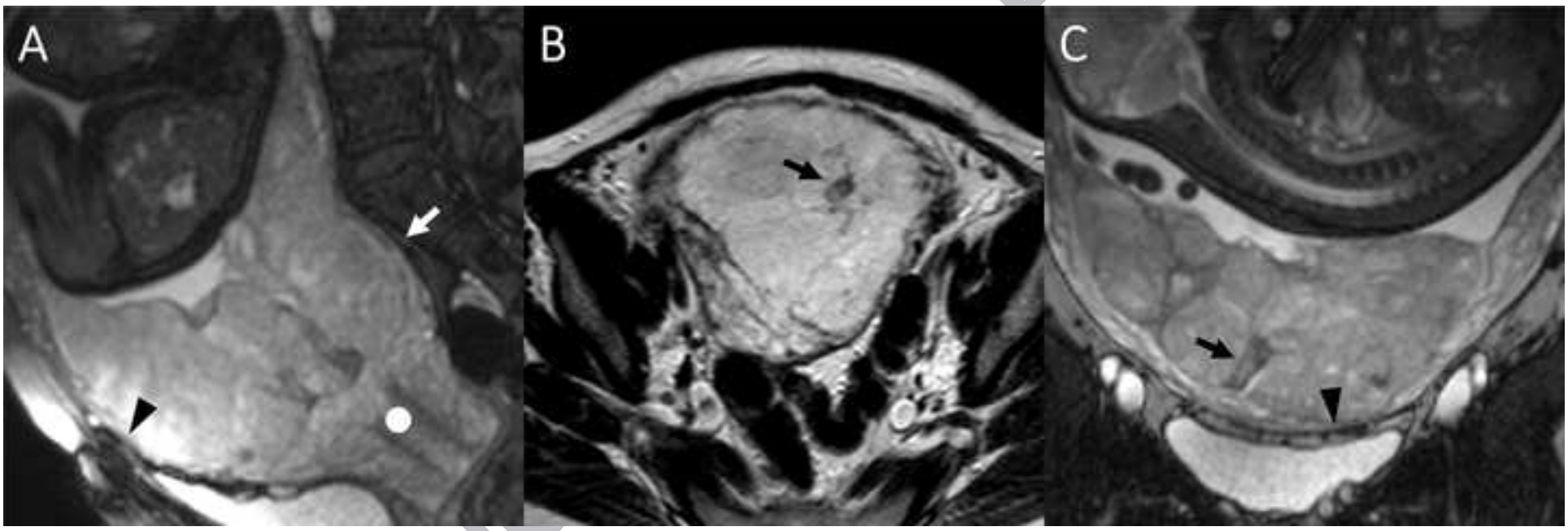

Fig. 4

Click here to access/download;Figure;4AB.jpg

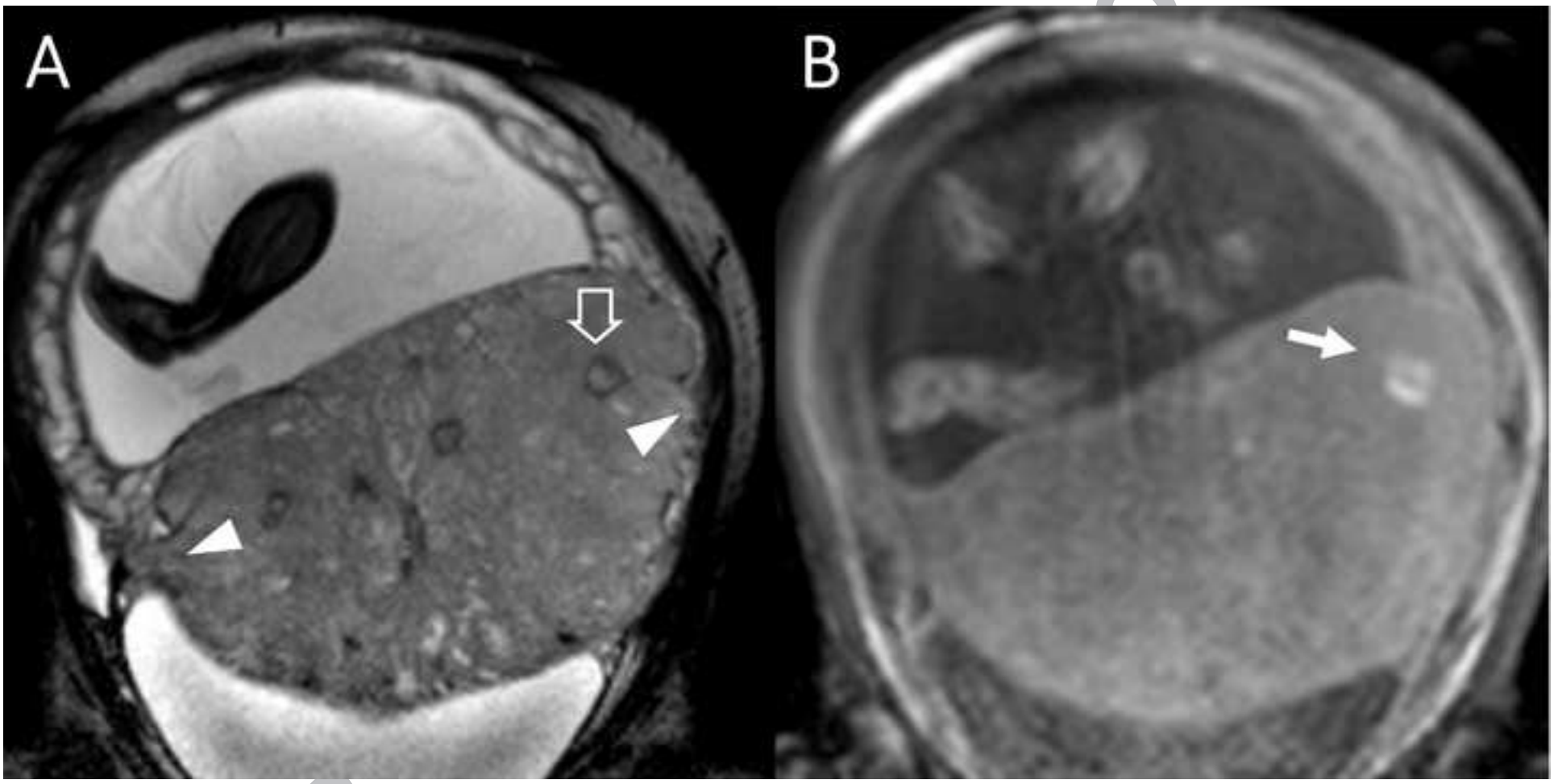

Table - changes marked

Table 1: Exam protocol

Sequence (name)	Sequence detail	Acquired planes
single-shot turbo spin-echo T2-weighted (TSE)	RT/ET: 3293/80 ms Slice thickness: 5 mm Acquisition matrix: 264x220	Sagittal Axial Coronal
three-dimensional high-resolution isotropic volume T1-weighted fat-saturated (THRIVE)	RT/ET: 3.6/1.69 ms. Slice thickness: 6 mm Acquisition matrix: 124x110	Axial Sagittal
Steady-state free precession sequences (balanced turbo field-echo BTFE)	RT/ET: 3.5/1.77 ms Slice thickness: 5 mm Acquisition matrix: 272x212	Sagittal Axial Coronal
DWI; EPI imaging single shot	RT/ET: 3.584/71 ms Slice thickness: 5 mm Acquisition matrix: 104x85 B values: 0-400-800	Axial

Table 2: Study population.

	All patients (26)	Non-IP (13)	IP (13)	PA / PI (10)	PP (3)
Age (years)	36.24 (± 6.16)	37.15 (±5.26)	35.33 (±7.05)	37.45 (± 6.47)	28.29 (±3.54)
Gestational age (weeks)	33.81 (± 5.36)	35.00 (±2.35)	32.62 (±7.16)	32.10 (±7.84)	34.33 (±5.03)
Previous pregnancies	3.35 (± 2.53)	2.46 (±1.20)	4.23 (±3.19)	4.80 (±3.43)	2.33 (±1.15)
Parity	1.54 (± 1.75)	0.92 (±1.12)	2.15 (±2.08)	2.40 (±2.27)	1.33 (±1.15)
Uterine surgery °	1.23 (±1.11)	1.00 (±1.08)	1.46 (±1.13)	1.60 (±1.17)	1.00 (±1.00)
BMI *	23.90 (±17.52)	23.82 (±5.94)	23.98 (±5.91)	24.22 (±6.26)	23.18 (±22.95)

Table 3: Accuracy and interrater agreement of MRI.

	SEN (%)	SPEC (%)	AUROC	PPV (%)	NPV (%)	Cohen's K
MRI	100 75,3 - 100	92,31 64,0 - 99,8	0,962 0,804 - 0,999	92,9 66,1 - 99,8	100 73,5 - 100	1,000 1,000 - 1,000
MRI of placenta percreta	66,7 9,4 - 99,2	95,7 78,1 - 99,9	0,812 0,611 - 0,937	66,7 9,4 – 99,2	95,7 78,1 - 99,9	0,708 0,336 - 1,000
Uterine Bulging	92,3 64,0 - 99,8	84,6 54,6 - 98,1	0,885 0,698 - 0,976	85,7 67,2 - 98,2	91,7 61,5 - 99,8	0,766 0,519 - 1,000
Placental Heterogeneity	100 75,3 - 100	100 75,3 - 100	1,000 0,868 - 1,000	100 75,3 - 100	100 75,3 - 100	0,769 0,524 - 1,000
Dark intraplacental bands	84,6 54,6 - 98,1	76,9 46,2 - 95,0	0,808 0,606 - 0,934	78,6 49,2 - 95,3	83,3 51,6 - 97,9	1,000 1,000 - 1,000
Hyperintense placental lacunae	61,5 31,6 - 86,1	58,3 27,7 - 84,8	0,599 0,386 - 0,788	61,5 31,6 - 86,1	58,3 27,7 - 84,8	0,516 0,183 - 0,849
Interruption of the myometrium	84,6 54,6 - 98,1	100 75,3 - 100	0,923 0,749 - 0,991	100 71,5 - 100	86,7 59,5 - 98,3	0,846 0,643 - 1,000
Interruption of inner myometrial layer	100 75,3 - 100	61,5 31,6 - 86,1	0,808 0,606 - 0,934	72,2 46,5 - 90,3	100 63,1 - 100	0,462 0,100 - 0,824
Implant on uterine scar	53,9 25,1 - 80,8	100 75,3 - 100	0,769 0,564 - 0,910	100 59,0 - 100	68,4 43,4 - 87,4	0,698 0,391 - 1,000
Bladder tenting	38,5 13,9 - 68,4	92,31 64,0 - 99,8	0,654 0,443 - 0,828	83,3 35,9 - 99,6	60,0 36,1 - 80,9	0,539 0,195 - 0,883

Table 4: Efficacy of interventional radiology assistance of the delivery

	IR-A (11) mean	IR-NA (3) mean	Difference	95% C.I. of the difference		P
Blood loss (ml)	1763.64 (±805.32)	3033.33 (±57.74)	1269.70	225.87	2313.53	0.0106
Hb lost in operating room (g)	-1.59 (±0.96)	-1.37 (±1.99)	0.22	-1.47	1.91	0.3894
Red cells transfusion (ml)	305.45 (±472.79)	1100.00 (±173.20)	794.55	173.89	1415.20	0.0082
Days in ICU (n)	1.00 (±0.77)	3.00 (±2.65)	2.00	0.17	3.83	0.0174
Hospitalization (days)	12.00 (±9.22)	41.67 (±42.44)	29.67	2.33	57.00	0.0179
Risk of transfusion (rr)	0.3636	1.0000	2.78			0.051
Risk of hysterectomy (rr)	0.8182	0.6667	0.81			0.571

Commented [A1]: Added RR of being hysterectomized in accordance to comment M of reviewer 2.

Table 1: Exam protocol

Sequence (name)	Sequence detail	Acquired planes
single-shot turbo spin-echo T2-weighted (TSE)	RT/ET: 3293/80 ms Slice thickness: 5 mm Acquisition matrix: 264x220	Sagittal Axial Coronal
three-dimensional high-resolution isotropic volume T1-weighted fat-saturated (THRIVE)	RT/ET: 3.6/1.69 ms. Slice thickness: 6 mm Acquisition matrix: 124x110	Axial Sagittal
Steady-state free precession sequences (balanced turbo field-echo BTFE)	RT/ET: 3.5/1.77 ms Slice thickness: 5 mm Acquisition matrix: 272x212	Sagittal Axial Coronal
DWI; EPI imaging single shot	RT/ET: 3.584/71 ms Slice thickness: 5 mm Acquisition matrix: 104x85 B values: 0-400-800	Axial

Table 2: Study population.

	All patients (26)	Non-IP (13)	IP (13)	PA / PI (10)	PP (3)
Age (years)	36.24 (± 6.16)	37.15 (±5.26)	35.33 (±7.05)	37.45 (± 6.47)	28.29 (±3.54)
Gestational age (weeks)	33.81 (± 5.36)	35.00 (±2.35)	32.62 (±7.16)	32.10 (±7.84)	34.33 (±5.03)
Previous pregnancies	3.35 (± 2.53)	2.46 (±1.20)	4.23 (±3.19)	4.80 (±3.43)	2.33 (±1.15)
Parity	1.54 (± 1.75)	0.92 (±1.12)	2.15 (±2.08)	2.40 (±2.27)	1.33 (±1.15)
Uterine surgery °	1.23 (±1.11)	1.00 (±1.08)	1.46 (±1.13)	1.60 (±1.17)	1.00 (±1.00)
BMI *	23.90 (±17.52)	23.82 (±5.94)	23.98 (±5.91)	24.22 (±6.26)	23.18 (±22.95)

Table 3: Accuracy and interrater agreement of MRI.

	SEN (%)	SPEC (%)	AUROC	PPV (%)	NPV (%)	Cohen's K
MRI	100 75,3 - 100	92,31 64,0 - 99,8	0,962 0,804 - 0,999	92,9 66,1 - 99,8	100 73,5 - 100	1,000 1,000 - 1,000
MRI of placenta percreta	66,7 9,4 - 99,2	95,7 78,1 - 99,9	0,812 0,611 - 0,937	66,7 9,4 – 99,2	95,7 78,1 - 99,9	0,708 0,336 - 1,000
Uterine Bulging	92,3 64,0 - 99,8	84,6 54,6 - 98,1	0,885 0,698 - 0,976	85,7 67,2 - 98,2	91,7 61,5 - 99,8	0,766 0,519 - 1,000
Placental Heterogeneity	100 75,3 - 100	100 75,3 - 100	1,000 0,868 - 1,000	100 75,3 - 100	100 75,3 - 100	0,769 0,524 - 1,000
Dark intraplacental bands	84,6 54,6 - 98,1	76,9 46,2 - 95,0	0,808 0,606 - 0,934	78,6 49,2 - 95,3	83,3 51,6 - 97,9	1,000 1,000 - 1,000
Hyperintense placental lacunae	61,5 31,6 - 86,1	58,3 27,7 - 84,8	0,599 0,386 - 0,788	61,5 31,6 - 86,1	58,3 27,7 - 84,8	0,516 0,183 - 0,849
Interruption of the myometrium	84,6 54,6 - 98,1	100 75,3 - 100	0,923 0,749 - 0,991	100 71,5 - 100	86,7 59,5 - 98,3	0,846 0,643 - 1,000
Interruption of inner myometrial layer	100 75,3 - 100	61,5 31,6 - 86,1	0,808 0,606 - 0,934	72,2 46,5 - 90,3	100 63,1 - 100	0,462 0,100 - 0,824
Implant on uterine scar	53,9 25,1 - 80,8	100 75,3 - 100	0,769 0,564 - 0,910	100 59,0 - 100	68,4 43,4 - 87,4	0,698 0,391 - 1,000
Bladder tenting	38,5 13,9 - 68,4	92,31 64,0 - 99,8	0,654 0,443 - 0,828	83,3 35,9 - 99,6	60,0 36,1 - 80,9	0,539 0,195 - 0,883

Table 4: Efficacy of interventional radiology assistance of the delivery

	IR-A (11) mean	IR-NA (3) mean	Difference	95% C.I. of the difference		P
Blood loss (ml)	1763.64 (±805.32)	3033.33 (±57.74)	1269.70	225.87	2313.53	0.0106
Hb lost in operating room (g)	-1.59 (±0.96)	-1.37 (±1.99)	0.22	-1.47	1.91	0.3894
Red cells transfusion (ml)	305.45 (±472.79)	1100.00 (±173.20)	794.55	173.89	1415.20	0.0082
Days in ICU (n)	1.00 (±0.77)	3.00 (±2.65)	2.00	0.17	3.83	0.0174
Hospitalization (days)	12.00 (±9.22)	41.67 (±42.44)	29.67	2.33	57.00	0.0179
Risk of transfusion (rr)	0.3636	1.0000	2.78			0.051
Risk of hysterectomy (rr)	0.8182	0.6667	0.81			0.571